Evaluation of Remediation Techniques for Circular Holes in the Webs of Wood I-Joists

Tiberiu Polocoser, A.M.ASCE[1]; Thomas H. Miller, M.ASCE[2]; and Rakesh Gupta, M.ASCE[3]

Abstract: Remediation methods and strength predictions were evaluated for wood I-joists with single, circular holes in the webs, leaving utilities in place. A full-scale bending test using four equally spaced point loads was applied to three depths of joists with varying flange widths and span lengths of 4.88 and 2.44 m. Failure modes for long-span joists without holes were in the flanges in tension, compression, or lateral buckling, but once a hole was introduced, the majority failed in shear. The curved beam approach and manufacturers software were used to predict strength. Seven remediation techniques were investigated initially, and remediation effectiveness was evaluated on the basis of strength, stiffness, and ease of installation/cost. The oriented strand board (OSB) collar remediation worked very well and returned 8 of 12 series of joists to a strength statistically equivalent to the "no hole" condition. The OSB collar was not quite as effective in returning stiffness to the joists but was easier to install and less expensive than a laminated strand lumber patch. **DOI:** 10.1061/(ASCE)MT.1943-5533.0000737. © *2013 American Society of Civil Engineers.*

CE Database subject headings: Wood structures; Joints; Holes; Webs (structural).

Author keywords: Wood structures; Joists; Holes.

Downloaded from ascelibrary.org by OREGON STATE UNIVERSITY on 06/19/17. Copyright ASCE. For personal use only; all rights reserved.

Introduction

There are various scenarios which arise throughout the construction process that may require a hole to be made in a structural member. In residential construction, the gypsum wallboard of the ceiling is often attached to the bottom of the floor/roof beams. In commercial construction, there can be a false/hanging ceiling, allowing for space between the structural members and the ceiling. There may also be a floor-to-floor height limit the architect is trying to achieve and no space left between the ceiling and the structural members. This condition will almost certainly cause the building utilities, plumbing, and heating ventilation and air conditioning (HVAC) ducts to be placed parallel to the structural members or, in the worst case, perpendicular and through the member. An optimal situation occurs when the mechanical engineer works in collaboration with the architect and structural engineer to locate beam penetrations. The next most favorable case is when a question is received from the jobsite before a beam penetration is made. Fig. 1(a) is an example of the worst-case scenario, in which beam penetrations are made on the jobsite by a subcontractor, and then the structural engineer is asked to check whether the condition is allowable.

[1]Research Fellow, Technische Universitat Braunschweig, iBMB-FG Organische Baustoffe und Holzwerkstoffe, Braunschweig 38106, Germany; formerly, Graduate Student, Dept. of Wood Science and Engineering, School of Civil and Construction Engineering, Oregon State Univ., Corvallis, OR 97331. E-mail: polocose@gmail.com

[2]Associate Professor, School of Civil and Construction Engineering, Oregon State Univ., Corvallis, OR 97331 (corresponding author). E-mail: thomas.miller@oregonstate.edu

[3]Professor, Dept. of Wood Science and Engineering, Oregon State Univ., Corvallis, OR 97331. E-mail: rakesh.gupta@oregonstate.edu

Note. This manuscript was submitted on July 26, 2012; approved on November 16, 2012; published online on November 20, 2012. Discussion period open until May 1, 2014; separate discussions must be submitted for individual papers. This paper is part of the ***Journal of Materials in Civil Engineering***, Vol. 25, No. 12, December 1, 2013. © ASCE, ISSN 0899-1561/2013/12-1898-1909/$25.00.

I-joist manufacturers produce literature on the appropriate uses for their products according to testing done following ASTM D5055 (ASTM 2012) and Wood I-Joists Manufacturers Association (WIJMA 1999) guidelines. Among the literature provided are hole charts indicating the sizes and shapes of holes allowed in certain locations along an I-joist. They also indicate the maximum number of holes allowed per span and the spacing required between holes. Fig. 1(a) shows oversized holes that are spaced too closely together, and Fig. 1(b) is an example from the same jobsite where too many holes are located in the web. Although the hole charts describing allowable hole conditions are readily available for the end-user, this problem persists regularly.

The difficulty with addressing the question from the field is the lack of detailed guidance from building codes, design guides, and textbooks for wood beams with a hole. To provide a response, the engineer needs to calculate a stress resulting from the expected loading condition and hole geometry and compare this to an allowable stress for the material. If the condition is deemed unacceptable, a costly option is to remove the utilities and the joists and replace them with new joists and place the utilities in an acceptable location.

Design guides and textbooks do not provide much guidance, but that is not to say the problem has not been covered in research. Engineering students are often taught about stress concentrations for the simplest case of an infinite plate with a hole under uniaxial tension. The solutions to most circular hole problems are shown using a polar coordinate system for ease of presentation, and stresses are represented by $\sigma_{\text{tangential}}$ and σ_{radial}. σ_{radial} is a minor contributor to the stress state at the boundary of a hole, and the results are generally described in terms of $\sigma_{\text{tangential}}$. For the problem of uniaxial stress, the resulting $\sigma_{\text{tangential}}$ on the axis perpendicular to the applied tension is three times larger than the average applied stress. Smith (1944) found that for Sitka spruce (solid sawn lumber) under the same loading condition, the stress concentration is 5.84 as opposed to 3 for an isotropic material such as steel. Although the stresses are higher in wood, the stress attenuates more quickly from the peak. Smith (1944) and

J. Mater. Civ. Eng., 2013, 25(12): 1898-1909

Downloaded from ascelibrary.org by OREGON STATE UNIVERSITY on 06/19/17. Copyright ASCE. For personal use only; all rights reserved.

(a) (b)

Fig. 1. Examples of holes in wood I-joists: (a) holes spaced too closely; (b) multiple utility holes

Lewis et al. (1944) worked in conjunction and determined that although $\sigma_{tangential}$ is highest at 90° from the axis of uniaxial tension, $\sigma_{tangential}$ at an angle of 78° actually caused failure because $\sigma_{tangential}$ at 78° is greater than the tension perpendicular to the grain capacity of the wood. This angle at failure will be different for oriented strand board (OSB) web material, corresponding to the maximum tangential tension stress [discussed further in Appendix A of Polocoser (2012)].

In wood beam design, a cross section is examined to find the maximum shear and bending stresses. For a wood I-joist, the flange modulus of elasticity (MOE) is much stiffer than the web MOE, and bending stresses are distributed according to the respective stiffnesses. Fig. 2(b) helps visualize the effect of the hole on the stresses in the cross section. The shear stress returns to zero at the boundary of the hole because of the traction-free surface, but there is a higher peak shear stress than for a homogeneous cross section (indicated with the broken lines). The bending stress is also shown in comparison with a homogeneous section. St. Venant's principle is seen here as the stresses farther away from the concentration at the boundary of the hole return to the usual strength of materials linear distribution. Fig. 3 represents the $\sigma_{tangential}$ stress state at the boundary of hole shown in Fig. 2(a), developing because of significant shear stresses in the web. The location of the maximum $\sigma_{tangential}$ tension stress as OSB is weaker in tension than in compression, and failure will occur because of this maximum stress. The nonuniform distribution of flakes between layers and within a layer in OSB further complicates the situation and makes a hole in an OSB web a virtually intractable analytical problem to solve, which is why solutions are found by using finite-element methods or approximate analysis techniques.

Bower (1966) first used a Vierendeel truss model for an approximate analysis of the stresses at a circular hole boundary. This method was used and compared in subsequent research by Knostman et al. (1977), Wang (1994), Cheng (1996), and Afzal et al. (2006). The Vierendeel truss model showed good agreement with test results but had limitations in its applicability. The model assumed a rectangular hole, which causes greater stress concentrations than the circular hole. When the hole is very large and there is little web remaining, the section would no longer act like a Vierendeel truss; therefore, the model was no longer accurate. Wang (1994) recommended that remediation techniques should be investigated for holes in the web. Cheng (1996) was the first to apply two remediation techniques for a single hole in the web of a wood I-joist but with only one replicate for each technique. The one effective remediation technique of using OSB on both sides of the web improved the load capacity by 57% from the condition with a hole. The OSB patch was placed on both sides of the web, and completely around the hole like the OSB collar in this research but did not have a cut that would allow access to place the patch above and below the square hole and allow the patch to go around utilities. Chan and Redwood (1974) first incorporated the Winkler-Bach curved beam approach (Huston and Josephs 2009) to approximate the stress at the hole boundary in a steel I-beam. This method was an improvement because it incorporated the stress concentration occurring at the hole and was also applicable to holes eccentric from the neutral axis. Pirzada et al. (2008) made this method applicable to wood I-joists by incorporating fracture mechanics properties of the web section.

Along with examining compromises to the strength from web holes, research on the effective stiffness was conducted by Clinch (1993) for I-joists with holes. An increasing number of holes were placed along the centerline of the joists to see how the stiffness was affected. Clinch (1993) concluded that the maximum decrease was 8% for the worst-case scenario. Morrissey et al. (2009) also

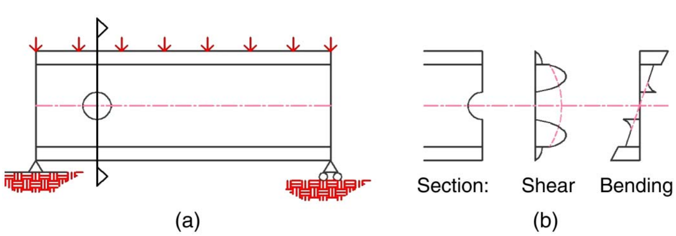

Fig. 2. (a) Simply supported wood I-joist with uniform load; (b) stresses at the cross section

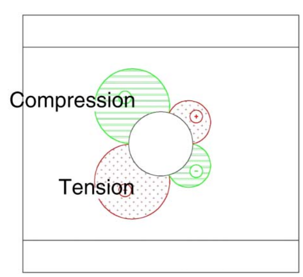

Fig. 3. Tangential stress distribution near hole in web

J. Mater. Civ. Eng., 2013, 25(12): 1898-1909

conducted experimental tests on joists with multiple holes. They looked at a remediation technique using a steel angle between the web and flange and found there was a benefit, but "alternative retrofits should be developed with consideration given to the ease of installation and materials readily available to the contractor on site."

Finally, recent research on modeling and behavior of wood I-joists is explored in Zhu et al. (2005a, b, 2007) and Guan and Zhu (2009).

Objectives

The main objectives of this study were to

1. Evaluate experimentally methods to remediate a wood I-joist with a single web hole.
2. Compare test results to approximate analysis methods predicting the failure load of a joist with a hole.
3. Provide additional information on practical methods to increase the capacity of a wood I-joist with a hole in the web while leaving the utilities and joist in place. This effort is designed to complement research by Cheng (1996) and Morrissey et al. (2009).
4. Examine the effective stiffness loss caused by a hole and effective stiffness with the methods of remediation. Stiffness generally governs the design of I-joists as a serviceability concern.
5. Evaluate remediation methods for ease of installation and cost.

Materials and Methods

Specimens

Sampling of joists was according to Section 4.3.3 of ASTM D2915-10 (ASTM 2010b). The population of joists represents a variety of different types in the product line, and samples were collected as they would be applied in the end use. Randomization of replicates was made from each of the bundles of joists. Flanges were made from Douglas Fir laminated veneer lumber (LVL) with flange-to-flange finger joints occurring at 1,219 mm (4 ft) on center (o.c.). Webs were manufactured with Aspen flakes with a web-to-web finger joint occurring at 1,219 mm (4 ft) o.c., alternating with the flange-to-flange joints. The OSB flake orientation is 90° from the longitudinal neutral axis as visible from the outer layers. Flake orientation for interior layers and density is proprietary information. Table 1 provides a detailed description of the joist dimensions and labeling for the different series of tests. In the period from manufacture to delivery, joists were stored in a weather wrapping in a dry outdoor condition. Any changes in relative humidity were assumed to be equal for each of the series of joists tested. Upon arrival to the Gene D. Knudson Wood Engineering Laboratory at Oregon State University, the joists were set outside in a dry condition until mechanical testing could begin. Although the joists underwent changes in weather, which could influence the strength and stiffness compared with new-condition joists used for product testing, the joists should be useful for drawing conclusions in comparison with one another.

Test Setup

ASTM D5055 Section 6.4.3 (ASTM 2012) specifies a three- or four-point bending test, whereas WIJMA (1999) Section 3.4.3 specifies a three-point bending test. The testing setup created was a six-point bending test to better simulate the most common loading condition of a distributed load. Although the three-point bending test creates the largest moment, the six-point bending test allowed for different values of constant shear between loading points and increased lateral restraint provided by the shorter unbraced lengths. Loading points were spaced at a distance of $2L/10$, where L is the center-to-center span of the joist between the load cells. Tests were conducted on the floor, with the I-joist laying flat and parallel to the floor. Fig. 4 illustrates the entire testing setup. Testing was displacement controlled, and there were two hydraulic cylinders with 102 mm (4 in.) bores. Their capacity was a maximum 17.24 MPa (2,500 psi), which provided a maximum loading of 139.7 kN (31.4 kips) per cylinder. Load was transmitted to a spreader bar and then to a $102 \times 102 \times 20$ mm ($4 \times 4 \times 3/4$ in.) steel plate. This plate was designed to be large enough to ensure that no crushing failures occurred at the flange. The location of the hole, that was not permitted according to the manufacturer hole charts, was at $L/10$ from the left end for both the long- and short-span beams.

Fig. 5 shows the cross section of the testing apparatus. A wood shim was placed between the I-joist and the hollow structural section (HSS) rectangular tube to ensure that loading would be concentric with the middle of the joist and to help prevent lateral buckling. The testing setup is braced along the bottom completely by the laboratory floor and on the top by large steel channels, bolted in place at quarter points of the span.

The shear (V) at the hole location was $2P$, where P is the point load, and the moment (M) was $PL/5$. The shear:moment (V:M) ratio at the hole location was $10/L$; for the long-span tests, 0.625, and for the short-span tests, 1.25. The span-to-depth ratio recommended by ASTM D5055-12 (ASTM 2012) is between 17:1 and 21:1, but the testing was limited by the shortest test specimens

Table 1. I-Joist Dimensions

Series	Joist depth, mm (in.)	Flange width, mm (in.)	Flange depth, mm (in.)	Web thickness, mm (in.)	Span, mm (in.)	Span-depth ratio	Hole diameter, mm (in.)	Hole diameter/joist depth (%)
A	241 (9.5)	44 (1.75)	32 (1.25)	9.5 (0.38)	4,877 (192)	20:1	152 (6)	63
B	356 (14)	59 (2.31)	35 (1.38)	9.5 (0.38)	4,877 (192)	14:1	203 (8)	57
C	356 (14)	89 (3.50)	35 (1.38)	11 (0.44)	4,877 (192)	14:1	203 (8)	57
D	406 (16)	53 (2.06)	32 (1.25)	9.5 (0.38)	4,877 (192)	12:1	203 (8)	50
E	406 (16)	59 (2.31)	35 (1.38)	9.5 (0.38)	4,877 (192)	12:1	229 (9)	56
F	406 (16)	89 (3.50)	35 (1.38)	11 (0.44)	4,877 (192)	12:1	203 (8)	50
G	241 (9.5)	44 (1.75)	32 (1.25)	9.5 (0.38)	2,439 (96)	10:1	152 (6)	63
H	356 (14)	59 (2.31)	35 (1.38)	9.5 (0.38)	2,439 (96)	7:1	203 (8)	57
I	356 (14)	89 (3.50)	35 (1.38)	11 (0.44)	2,439 (96)	7:1	203 (8)	57
J	406 (16)	53 (2.06)	32 (1.25)	9.5 (0.38)	2,439 (96)	6:1	203 (8)	50
K	406 (16)	59 (2.31)	35 (1.38)	9.5 (0.38)	2,439 (96)	6:1	203 (8)	50
L	406 (16)	89 (3.50)	35 (1.38)	11 (0.44)	2,439 (96)	6:1	203 (8)	50

J. Mater. Civ. Eng., 2013, 25(12): 1898-1909

Downloaded from ascelibrary.org by OREGON STATE UNIVERSITY on 06/19/17. Copyright ASCE. For personal use only; all rights reserved.

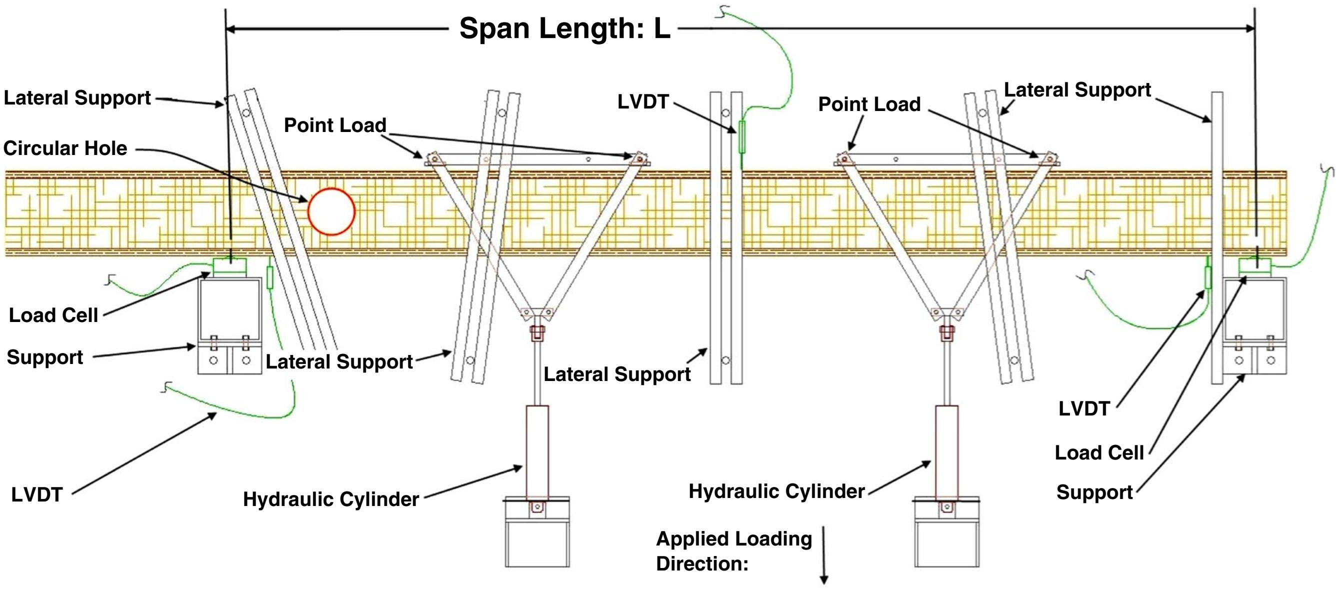

Fig. 4. Testing setup plan view

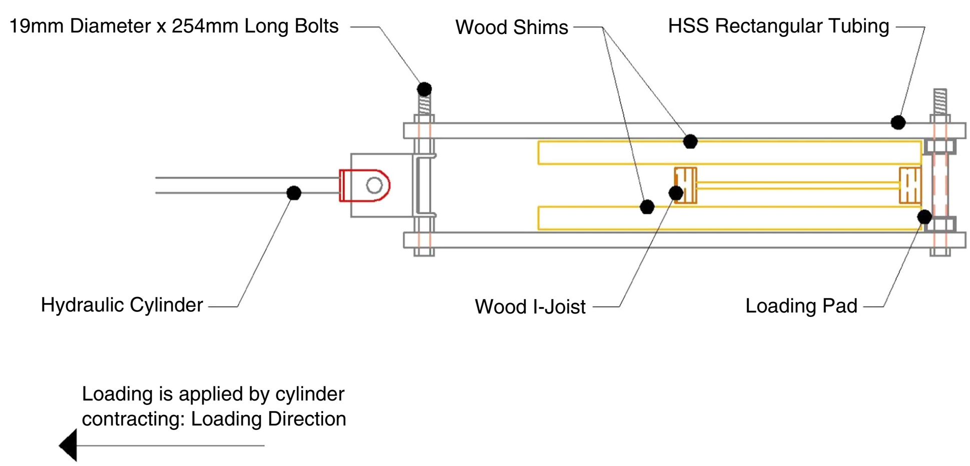

Fig. 5. Testing setup cross section

supplied. Span-to-depth ratios for each test series are provided in Table 1.

Data Acquisition

Two sets of deflection data were acquired from the test setup. The deflection of the joist was measured at the midspan by a linearly variable differential transformer (LVDT) and also at the ends of the joist. The LVDTs at the ends of the joist were placed to verify that no crushing was occurring at the ends of the specimen.

Load data were measured by using 29 kN (20 kips) maximum capacity load cells at each end of the joist.

The load and deflection data were collected by using *LabView 2010*. The loading rate for the long-span tests was set to 13 min/min (0.5 in./min) and 4 min/min (0.15 in./min) for the short-span tests to comply with the ASTM D5055 (ASTM 2012) requirement to not cause failure in less than a minute. Data were recorded in 0.2-s increments.

Predictions

Predictions of failure load were made by using two methods. The first method used free software created by I-joist manufacturers and provided online. This method would be the first step a practicing engineer has at his/her disposal for determining the capacity of the joist. This method was used to estimate the strength for the control condition with no hole and then also to introduce a hole and determine the allowable capacity. For one I-joist manufacturer, the software would not give the capacity of the joist at the hole location if the location was too close to the support. For the other software, an error notice appeared indicating that the hole was too close to a support, but it still provided a failure load at the hole location. Allowable loads from the software were

J. Mater. Civ. Eng., 2013, 25(12): 1898-1909

Downloaded from ascelibrary.org by OREGON STATE UNIVERSITY on 06/19/17. Copyright ASCE. For personal use only; all rights reserved.

Downloaded from ascelibrary.org by OREGON STATE UNIVERSITY on 06/19/17. Copyright ASCE. For personal use only; all rights reserved.

multiplied by a factor of safety of 3 to compare to the testing results. Per ASTM D5055 Section 6.4.3.4 (ASTM 2012), "moment capacity shall be based on the lower 5% tolerance limit with 75% confidence divided by 2.1." A factor of 3 was used to compensate for testing specimens representing values closer to the mean of the distribution and not the lowest 5% value. The factor of safety of 3 is better suited for a population with a coefficient of variation (COV) of approximately 20%. At the beginning of testing, the expected variability caused by the hole and the fixes was unknown.

The second method (Polocoser 2012) of predicting the failure load was an application of the curved beam–fracture mechanics approach developed by Pirzada et al. (2008). The maximum tension stress around the boundary of the hole will occur between 225° and 270°, when measuring counterclockwise from the longitudinal neutral axis of the joist. The procedure analyzes the stresses along the boundary of the hole between these angles. Applied load and internal shear force and moment at the cross section of the hole (assuming a cross section without a hole) are determined. Maximum $\sigma_{\text{tangential}}$ is then determined by using the Winkler Bach curved beam (Huston and Josephs 2009) method. Shear and moment at the cross section are decomposed and applied as an axial force and shear force acting through the centroid of the tee section created for the analysis. A characteristic length parameter measured from the boundary of the hole defines the length over which the tangential stresses will attenuate on the basis of a combination of material properties. Then, a function is calculated describing the stress as it attenuates from the peak at the boundary of the hole and the ratio P_{failure}:P_{applied}. After calculating the ratio for this range of angles, the minimum ratio value determines the angle at which failure is expected to occur. The load determined from this process was then multiplied by 3.0 to compare with the failure load from testing. The factor of safety of 3 is found in WIJMA (1999) Section 4.1 for joists tested with holes in the web.

This approximate method of determining the failure load was used for three test types: no hole, hole, and OSB collar. For the test type "no hole," the prediction procedure was applied to a very small hole of 10 mm (0.4 in.) to predict the failure load. The method was then applied as intended for the test type "hole." The method was finally also extended to test type "OSB collar" by tripling the thickness of the web of the joist (for OSB glued to both sides of the web) to determine whether the method could be applied to estimate the failure load with the patch.

Initial Testing

Full-scale testing in Series E was used initially to explore various remediation techniques and determine which methods of remediation to apply to the rest of the test series. Because of the limited number of I-joists, six replicates of each type were tested for each joist series. This is an insufficient number to make substantial claims for what should be used in the field (e.g., determining allowable properties), but it is enough to recognize the trends in the data and make initial recommendations from this first round of testing. According to ASTM D2915 Section 4.4.2 (ASTM 2010b), the required sample size should be between 20 and 30 replicates to draw strong conclusions for the population. The initial round of testing included the following test types:

1. Control group for each depth and flange width with no hole.
2. Control group with a circular hole larger than allowed by manufacturer charts, centered $L/10$ from the left end of the setup. L is measured as the center-to-center distance between the supports.

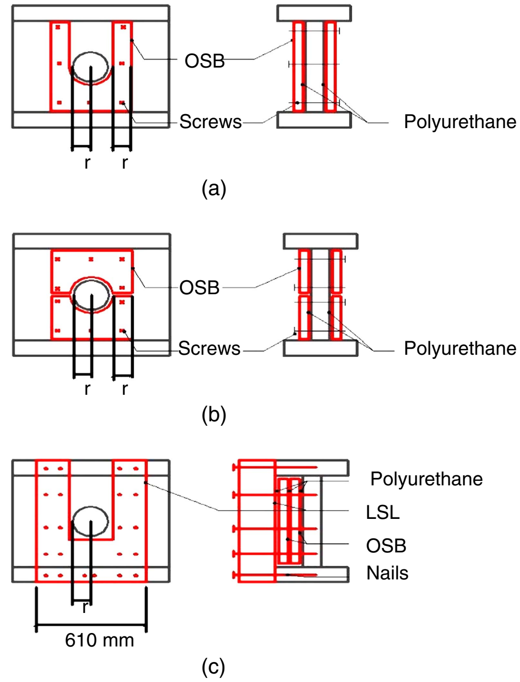

Fig. 6. (a) Tests 8 and 9; (b) Test 10; (c) Test 11

3. Joists with a circular hole of the same diameter but at an acceptable location according to the manufacturer's charts, centered $3L/10$ from the left end of the setup.
4. Loctite PL (Henkel, Dusseldorf, Germany) Premium polyurethane construction adhesive on the inside of the hole boundary and for an annular distance of 38 mm (1.5 in.) surrounding the hole.
5. Nominal 38×90 mm (2×4 in.) select structural Douglas Fir web stiffeners screwed to both sides of the hole and both sides of the web.
6. Same as Test 5 except with Loctite PL Premium polyurethane construction adhesive between the nominal 38×90 mm (2×4 in.) stiffeners and web.
7. 457 mm (18 in.) long Simpson CS 22 (Simpson Strong-Tie, Pleasanton, CA) metal straps nailed above and below the hole.
8. Two U-shaped OSB patches with West System (West System, Bay City, MI) three-part epoxy applied to both sides of the web are shown in Fig. 6(a). The patch was kept in place and pressure applied by seven Spax 5.2×51 mm (10×2 in.) course (Spax International GmbH, Enneptal, Germany), yellow, zinc-plated, steel, flat-head, combination wood screws while the epoxy set.
9. Same as Test 8 except PL Premium polyurethane adhesive instead of epoxy. The purpose for the U-Shape was the ease of installation and for increasing the cross-sectional area at the point of maximum tangential stress at the hole. It could be slid up and under a pipe without any difficulty. The patch was kept in place and pressure applied by seven Spax 5.2×51 mm (10×2 in.) course, yellow, zinc-plated, steel, flat-head, combination wood screws while the adhesive set.
10. Two collar-type OSB patches above and below the hole with PL Premium polyurethane adhesive applied to both sides of the web are shown in Fig. 6(b). The OSB was the same as that taken from the web of another I-joist. Each patch was kept in place and pressure applied by five Spax 5.2×51 mm (10×2 in.) course, yellow, zinc-plated, steel, flat-head, combination wood screws while the adhesive set for ten wood screws per replicate.

J. Mater. Civ. Eng., 2013, 25(12): 1898-1909

11. Laminated strand lumber (LSL) nailed to the top and bottom flange and an OSB backer between the 32 mm (1.25 in.) thick LSL and the web, with PL Premium polyurethane adhesive applied between each layer. The outer dimensions of LSL were the depth of the joist × 610 mm (24 in.). The OSB backer is the same as the OSB web of another I-joist. Bostich (Stanley Bostich, New Britain, CT) full round-head nails, 63 × 4 mm (2.5 × 0.131 in.), were applied with a pneumatic nail gun. There were 22 nails per replicate as shown in Fig. 6(c). This fix was similar to a method recommended by a manufacturer.

Test Types 4–11, described in additional detail in Polocoser (2012), were also tested for the large circular hole at an unacceptable location.

After the application of adhesives, joists were allowed to cure for 4 days inside the laboratory at 22°C and a relative humidity of 70% before they were tested. Nominal 2 × 4 (38 × 90 mm) web stiffeners were placed on both sides of the web at the reaction points to help eliminate bearing failures.

Results and Discussion

Of the 377 joists tested, 360 joists were reported after removing those with obvious errors. Six replicates were tested per type, but sometimes there were only five acceptable replicates. Table 2 provides the number of replicates for each test type. For Series E and G, there were additional experimental remediation techniques and a higher number of total tests. The results for mean failure load for these tests are found in Table 2, along with the coefficient of variation. Joist Series A–F were tested at a long span (4.8 m), and Series G–L were the same-size joists but tested at a shorter span (2.4 m). The purpose of having two span lengths was to evaluate the influence of shear and moment interaction as it affected the results for the effects of the hole and the respective methods of remediation. Shear and moment cause different stress states at the boundary of the hole. Because of this interaction of stresses, shear and moment cannot be examined separately, as is currently often assumed for simplicity in engineering practice.

Load-deflection data (Polocoser 2012) from testing joists in the long-span tests was linear until the sudden failure. If there was any lateral-torsional buckling of the specimen, the plots had a slight nonlinear curve at the end before failure. The overlaying of plots indicated a very uniform and consistent effective stiffness. The two most efficient test types (rehabilitation methods) based on the load capacity were selected from the initial round of testing to be implemented for the rest of the series. The adhesives for the OSB patches did not fail at the bond line between the web and the patch, and therefore were considered to have successfully transferred load and acted as one piece with the web around the boundary of the hole. Fig. 7 shows the Fisher's least-significant difference (LSD) 95% confidence intervals with $\alpha = 5\%$ for the initial round of testing. The standard deviations for each test type were very similar, possibly because of consistent engineered properties and consistent failure modes. Fisher's least-significant difference is a liberal method to estimate the 95% confidence intervals. An α of 5% indicates the probability of incorrectly accepting the results of the statistical analysis, or that the observed results occurred by chance.

U-shaped OSB patches (Test Types 8 and 9) increased the strength of the joists and were effective, but not as effective as the OSB collar (Test Type 10) and the side LSL (Test Type 11) patches used in later testing (Fig. 7). In the initial round of testing, a reciprocating saw was used to cut 229 mm (9 in.) diameter holes. This method of cutting holes was not very desirable or consistent, and the largest-size hole saw with 203 mm (8 in.) diameter was used to create the rest of the holes uniformly and to consider only the largest reasonably sized hole. The laboratory was continuously heated through the fall and winter to maintain the same temperatures for curing of adhesives.

Table 3 is a comparison of the predicted loads and the mean loads at failure for test types "no hole," "hole," and "OSB collar." The percentage difference is calculated as $(\text{test result-prediction})/\text{test result} \times 100\%$. A negative percentage difference is an overprediction (liberal) of failure load, and a positive percentage difference is an underprediction (conservative) of failure load.

From Table 3, the curved beam approximation method tends to overpredict the failure load for the "no hole" and "OSB collar" test types and slightly overpredict for the "hole" case. A direct average is measured from all of the results, and an average of the absolute values is also provided for comparison but does not indicate whether a prediction is conservative or liberal. This result is an indication of limits to the applicability of the method. This method may not be applicable to very small holes or to thicker OSB webs, as observed from the data and the results of Pirzada et al. (2008). Another reason for the discrepancy could have come from the fracture energy of the OSB for this particular product, which was different from the product tested by Pirzada et al. (2008). The fracture energy property of the web is required for input into the approximation. The critical fracture energy, G_c, is the strain energy release rate required per area for the crack to propagate to failure of the specimen. The value required for input was assumed, as suggested by Pirzada et al. (2008), as 2,400 $\mathrm{J/m^2}$. The method developed

Table 2. Mean Failure Loads

	2 No hole			3 Hole			4 OSB collar			Side LSL		
1 Series	kN (lbs)	N^a	COV (%)	kN (lbs)	N	COV (%)	kN (lbs)	N	COV (%)	kN (lbs)	N	COV (%)
A	15.1 (3,405)	6	12	13.5 (3,026)	6	9	14.7 (3,298)	6	10	13.9 (3,129)	6	9
B	38.2 (8,592)	6	9	21.9 (4,922)	6	9	38.8 (8,726)	6	6	37.6 (8,458)	6	12
C	48.9 (10,983)	6	13	54.9 (5,603)	6	7	39.8 (8,956)	6	9	42.4 (9,539)	5	7
D	36.6 (8,219)	6	11	27.4 (6,163)	6	16	33.1 (7,441)	6	19	33.0 (7,413)	6	10
E	43.3 (9,741)	5	7	25.3 (5,683)	5	3	40.6 (9,126)	6	5	38.3 (8,607)	6	11
F	57.3 (12,870)	6	14	30.8 (6,934)	6	7	55.6 (12,510)	6	5	50.1 (11,267)	6	3
G	32.3 (7,259)	6	13	14.5 (3,251)	4	11	18.0 (4,047)	6	4	24.3 (5,457)	6	9
H	51.8 (11,649)	6	9	21.5 (4,843)	6	13	40.8 (9,179)	6	8	37.8 (8,497)	4	3
I	56.2 (12,637)	6	11	24.3 (5,455)	6	12	38.3 (8,602)	6	8	46.6 (10,485)	6	7
J	54.5 (12,259)	7	8	30.3 (6,821)	6	9	52.0 (11,692)	6	11	46.8 (10,529)	6	8
K	50.8 (11,414)	6	6	29.2 (6,569)	6	15	52.1 (11,715)	6	9	50.6 (11,370)	6	7
L	53.1 (11,932)	6	13	29.4 (6,604)	6	15	48.0 (10,797)	6	13	45.6 (10,260)	6	18

[a]N = number of replicates.

Downloaded from ascelibrary.org by OREGON STATE UNIVERSITY on 06/19/17. Copyright ASCE. For personal use only; all rights reserved.

Downloaded from ascelibrary.org by OREGON STATE UNIVERSITY on 06/19/17. Copyright ASCE. For personal use only; all rights reserved.

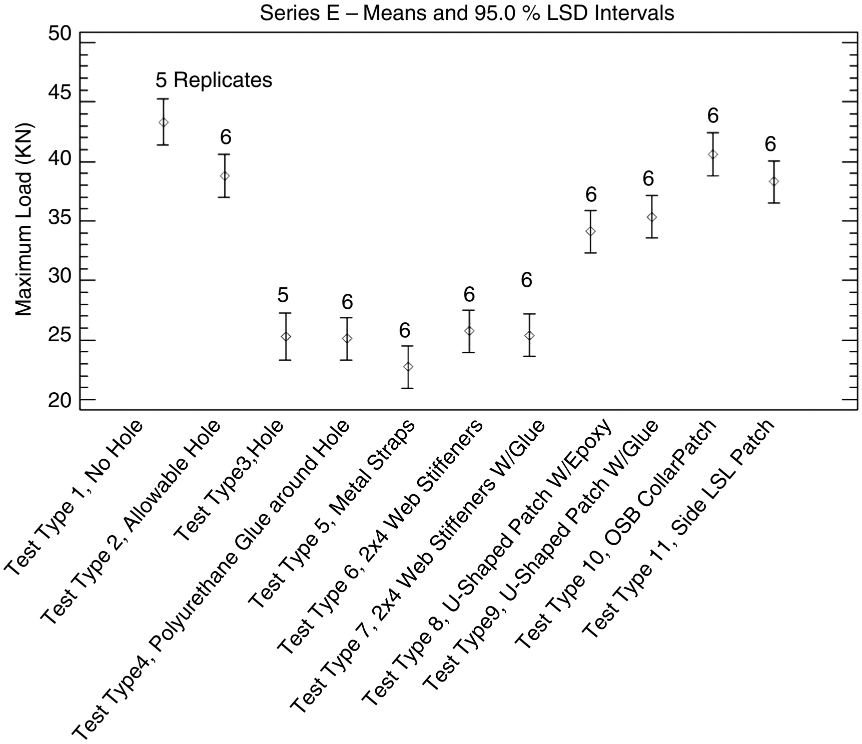

Fig. 7. Series E: Initial testing results

by Pirzada et al. (2008) performs well for the estimation of the large-hole condition used in the testing and is the most accurate compared with the other methods. The software packages calculate the capacity of the joist on the basis of shear capacity of the remaining web area above and below the hole, with a specified limit on the distance to a point load or support. The software packages also place a minimum shear close to the center of the span length, so for a uniformly distributed load, the design shear never reaches zero. Software 2 predicts the failure load reasonably well for the hole by using only the shear capacity of the web above and below the hole, but an error message indicates that it would fail because of the hole proximity to the support, and therefore the load would not be permissible for design by that manufacturer.

Table 3. Summary of Prediction Comparison for Failure Loads

Series	Curved beam (%) No hole	Curved beam (%) Hole	Curved beam (%) OSB collar	Software 1 (%) No hole	Software 1 (%) Hole	Software 2 (%) No hole	Software 2 (%) Hole
Long span							
A	−83	−22	−111	5	42	5	9
B	−46	−2	−36	−2	N/A	26	4
C	−34	−10	−63	7	N/A	−15	25
D	−65	−4	−124	20	N/A	12	−1
E	−38	5	−50	10	N/A	17	1
F	−23	−12	−62	21	N/A	−12	13
Short span							
G	−32	−17	−84	16	N/A	48	21
H	−7	−5	−35	22	N/A	11	2
I	−15	−15	−74	18	N/A	−2	23
J	−13	5	−47	26	N/A	−1	9
K	−17	0	−48	20	N/A	−4	5
L	−32	−19	−91	14	N/A	−19	9
Average	−34	−8	−69	15	42	6	10
Absolute average	34	10	69	15	42	14	10

Long-Span Tests

Failure Load Criterion

The failure load interaction plot is shown in Fig. 8. For Series A, the presence of a hole had a relatively small effect (11%) on the failure load. However, for Series B–F, the effect of the hole was more pronounced. For Series C, there was the largest (49%) loss in failure load caused by the presence of a hole. Also, greater loss in failure load was observed in joists with the same depth but increasing flange widths (for Series B–C and D–F), as failure loads for the control "no hole" case increased with the flange width. Table 4 summarizes the percentage difference of the mean failure loads and stiffnesses in comparison with the "no hole" test type. A large loss in strength from a hole could potentially result in a failure occurring in the field. An example that could cause failure to occur in the field is the possibility of a loading condition different from what was anticipated, such as a large point load placed over the location of the hole. Although this was not tested, it can be postulated from

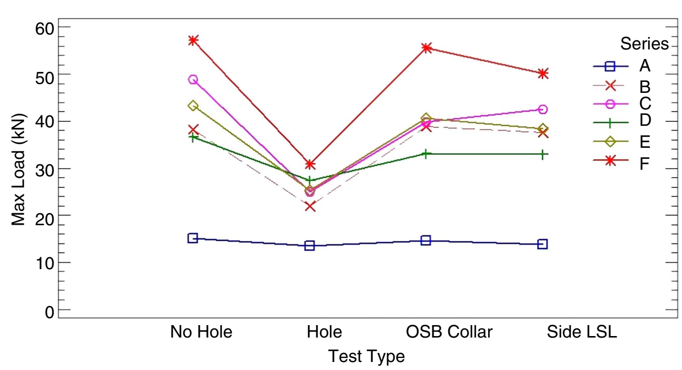

Fig. 8. Long-span failure load interaction plot

J. Mater. Civ. Eng., 2013, 25(12): 1898-1909

Table 4. Percentage Difference for Failure Load and Stiffness Compared with "No Hole" Case

	Failure load			Stiffness		
Series	Hole	OSB collar	Side LSL	Hole	OSB collar	Side LSL
A	−11	−3	−8	−4	−4	−4
B	−43	+2	−2	−1	+2	+1
C	−49	−18	−13	−6	+2	−3
D	−25	−9	−10	−3	0	−1
E	−42	−6	−12	−4	−3	−8
F	−46	−3	−12	−8	−8	−3
G	−55	−44	−23	−7	−6	+2
H	−58	−21	−25	−19	−8	+1
I	−57	−32	−17	−18	−8	−12
J	−42	−1	−11	+2	−5	−11
K	−42	+3	0	−8	0	+1
L	−45	−10	−14	−8	−8	−7

Table 5. Long-Span Comparison of Mean Failure Loads and Stiffnesses

	No hole–OSB collar		No hole–side LSL		OSB collar–side LSL	
Series	Failure load	Stiffness	Failure load	Stiffness	Failure load	Stiffness
A	x	x	x	x	x	x
B	x	x	x	x	x	x
C		x		x	x	
D	x	x	x	x	x	x
E	x	x			x	x
F	x			x		

x indicates no significant difference in failure load or stiffness.

experience and speculation of possible construction loads. This would cause a high shear stress different from the uniform loading condition considered in design. The plot in Fig. 8 for Series A is flat compared with the distinct shape of the line for Series F. The flat line of Series A indicates little effect of a hole as opposed to the dramatic loss in failure load for Series F. The crossing of the plots is a strong indication of an interaction of effects between the test series. An example of this is Series D crossing with Series B, C, and E. The crossing of lines and differences in the shapes of the interaction plots indicate the interaction of series effects; therefore, conclusions drawn for one series would not be valid to infer on the other series. For example, the observation for Series D is that a hole diameter of 50% of the total depth will cause a loss of 25% in failure load for a long-span joist, but because of the crossing of interaction plots, this type of conclusion cannot be applied to the other series. The small number of replicates may explain this interaction. More testing may be needed to verify that no errors were made in the testing of the "hole" test type for Series D. Each series must then be compared separately and conclusions drawn individually.

The mean failure loads Fisher's least-significant difference intervals were compared, and the results are provided in Table 5. The 95% confidence intervals have a range of approximately 5 kN (see Fig. 7), and the overlapping of intervals indicates where there is no significant difference between the test types. If more samples were taken, the confidence intervals would be smaller and would better represent the true differences between the test types. However, both patch types worked quite well to return the joist to a capacity that is statistically equivalent to a "no hole" condition.

Figs. 9(a–b) are examples of tension failures at the boundary of the hole occurring in the remediations, which were classified as ZW failures, which is a failure line that runs near to 45° through the web and does not involve a web-to-web joint. A complete list of the failure codes used can be found in Section X5.2 of ASTM D5055-12 (ASTM 2012).

For the long-span tests, the OSB collar remediation worked well when compared with the "no hole" test type, even resulting in flexural failure instead of shear failure. A comparison of the OSB collar to side LSL confidence intervals is made in the last column of Table 5 to show that there is no statistical difference between the two for all of the series except Series F in terms of failure load. The overlapping of confidence intervals between test types signifies no statistical difference between the test types. Differences between confidence intervals are presented in Appendix H of Polocoser (2012). Confidence intervals for each remediation are also used to make comparisons with the control "no hole" case, in the first two columns of Table 5 to examine the effectiveness of the patches. For all of the long-span series, there is substantial overlapping of these confidence intervals, demonstrating the remediation effectiveness. For the long-span testing, the OSB collar generally performed equivalently to the side LSL and better for Series F in terms of failure load. For Series C, both patches improved the failure load compared with the "hole" condition but not to a level statistically equivalent to the "no hole" condition.

Stiffness Criterion

For the long-span testing, there was very little difference in the stiffnesses of the joists with and without a hole, as shown in Table 4 and interpreted in Table 5. For Series A–F, the largest loss of

(a) (b)

Fig. 9. (a) Failure mode ZW for OSB collar; (b) failure mode ZW for LSL

J. Mater. Civ. Eng., 2013, 25(12): 1898-1909

Downloaded from ascelibrary.org by OREGON STATE UNIVERSITY on 06/19/17. Copyright ASCE. For personal use only; all rights reserved.

stiffness was 8%, which coincides with the results of Clinch (1993). The largest loss of stiffness was for the large depth, wide flange joists in Series F, in which shear is a significant contributor to overall deflection. The large and dense LSL patch provided the best method in Series F for returning the stiffness to a state similar to the "no hole" test type. The results presented in Table 5 show that there were generally no statistical differences between the "no hole" test type and the two methods of remediation, indicating that both methods are effective in returning stiffness to the joists.

Short-Span Tests

Failure Load Criterion

The short-span tests had a $V{:}M$ ratio double that of the long-span tests; therefore, the hole had a much greater impact on the load capacity because of the larger shear stress contribution in the web. The maximum loss in capacity was 58% for Series H (Table 4). The load-deflection data (Polocoser 2012) for the shorter-span tests were noticeably different from the long spans, with increased nonlinearity. For the short-span tests, there is more interaction of failure loads in Fig. 10, with more crossing of lines than for the long-span tests, indicating increased variation and influences of variables. The shape of the plot for Series G for a short depth, narrow flange joist is no longer relatively level like Series A, indicating the importance of the effects of holes on all joist types at a short span, in which shear is more dominant.

There were more abrupt losses of load during the loading, possibly because of "pop in," which happens when a fracture extends, releasing energy, and then loading continues to increase until the crack has run the full length from the edge of the hole to the web-to-flange connection. Another possibility for the decrease in load is when the developing crack reaches a point where there is adhesive missing between the patch and the web. However, in checking the adhesive bond line between the patch and web after testing, there were no signs of problems in bonding in this plane. Complete failure generally occurs along the web-to-flange connection because of delamination. Another reason or possibility for nonlinearity in load deflection is local failures of glued joints, which was difficult to observe during the testing procedure. Failures were increasingly difficult to identify and were generally not catastrophic like the bending failures of the long-span tests. For the short-span tests, the side LSL remediation specimens showed no failure in the LSL and only in the joist web, indicating that the loads were not being adequately transferred.

Comparing the means of the failure loads for the test types in Table 6, it is apparent that the two methods of remediation were not as effective as for the long-span tests over the range of joist types.

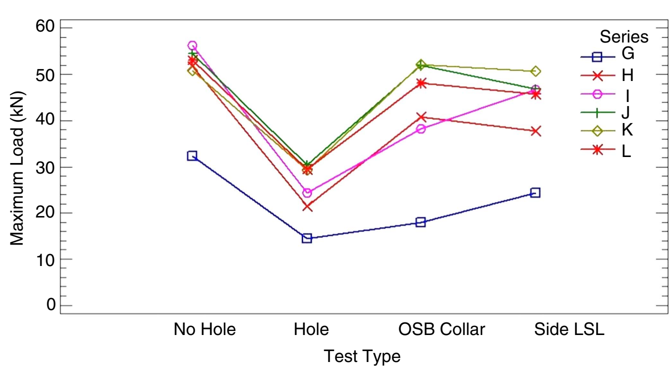

Fig. 10. Short-span failure load interaction plot

Table 6. Short-Span Comparison of Mean Failure Loads and Stiffnesses

	No hole–OSB collar		No hole–side LSL		OSB collar–side LSL	
Series	Failure load	Stiffness	Failure load	Stiffness	Failure load	Stiffness
G				x		
H				x	x	
I						x
J	x	x			x	x
K	x	x	x	x	x	x
L	x	x	x	x	x	x

x indicates no significant difference in failure load or stiffness.

This is expected because of the higher shear force carried through the web and patches. For Series G and I, the side LSL patch performed somewhat better than the OSB collar but not as well as a joist with no hole (Tables 4 and 6).

Stiffness Criterion

The stiffness of the joist is a major consideration in the design and use of wood I-joists and is often the controlling factor, especially for longer spans. Table 6 indicates the side LSL remediation technique was better at returning the stiffness for Series G and H but was not as effective as the OSB collar for Series J. The largest losses in effective stiffness for the holes were 19 and 18% for Series H and I, respectively (Table 4). The increased loss of stiffness compared with the long-span joists indicates an increased shear deflection caused by the loss of web material.

Failure Modes

The long-span test series experienced a majority of bending-type failures as expected. Most of the shear failures were confined to tests including a hole. Codes used to describe the failures were taken from ASTM D5055-12 (ASTM 2012). The most frequent failure mode for the long-span test was a tension failure in the flange with a subsequent bad bond failure in the web (FT-B). Another, less frequent failure mode for the long-span testing was flexural-torsional buckling, classified as FCB. With the addition of a hole, whether there was a remediation or not, the failure modes were predominantly in shear of the web at the boundary of the hole. The web failed in tension and then the crack would propagate until reaching the flange, when the web-to-flange adhesive would generally delaminate a certain distance until the testing was stopped.

Failure modes for the short-span tests were shear and bearing failures, such as web crippling (WC). The most predominant failure was ZW, which was a shear failure caused by the hole, as shown in Fig. 11(a). The average failure of the web occurred between the angles expected [225°–270°, where the values shown in Fig. 11(b) subtract 180° from these angles] from the behavior of stresses at the boundary of the hole. The distribution of failure angles for all of the tests is plotted in Fig. 11(b), which has an average of 57°. However, if there was a web-to-web connection at the boundary of the hole or very near the hole, the angle of fracture was affected according to the location of the connection.

The most common type of failure without a hole was ZJ, which is a shear failure but at the web-to-web joint. The joint caused most of the failures for the short-span tests without a hole but also significantly lowered the failure load when near a hole.

Ease of Repair and Cost

The ease of remediation installation is subjective and based on responses from several people in the laboratory who helped with

J. Mater. Civ. Eng., 2013, 25(12): 1898-1909

Downloaded from ascelibrary.org by OREGON STATE UNIVERSITY on 06/19/17. Copyright ASCE. For personal use only; all rights reserved.

(a)

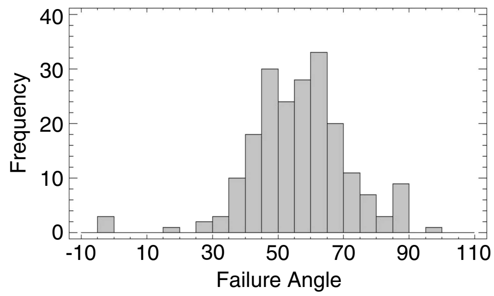

(b)

Fig. 11. (a) ZW failure at hole boundary; (b) distribution of failure angle for all tests

fabricating the test specimens. The OSB collar was significantly easier to cut from the material than the side LSL patch. The density of the LSL material made it difficult to cut and to nail through, even giving the pneumatic nail gun trouble. The LSL patch also required more adhesive between layers, making the process take longer than the OSB collar to install. A problem encountered while nailing the LSL patch was that the angle of the nail would on occasion come out the top of the flange instead of directly through the flange. This installation could be even more difficult in the field with limited space allowing for a nail gun.

The cost of the OSB collar is considerably less than the side LSL. The cost of the OSB collar applied to 10 of the deep joists was computed to be \$28.50 as opposed to \$54.57 for the side LSL, making the LSL patch approximately twice as expensive. These costs include the OSB, LSL, adhesives, screws, and nails. Sheets of OSB can be purchased without any difficulty from a lumber yard and are generally found on the jobsite. The LSL material is expensive in comparison and must be special ordered from the lumber yard. It is generally not kept in stock because of the limited uses on the jobsite. On the basis of the ease of installation and cost, the OSB collar is the most desirable option from the point of view of the installer.

Conclusions

Understanding the behavior of stresses at the boundary of a hole in a beam helps to understand the failure modes and methods that will be beneficial to remediate the hole. The approximate method developed by Pirzada et al. (2008) was used with relative ease and was the most accurate method for the simple hole condition but was not effective when extended to predictions of the failure load for the OSB collar patch or when used for a very small hole to predict the failure load for a "no hole" condition, as may be expected. This limitation is beneficial to know and may be improved in the future. Accurate material parameters such as fracture energy and tensile strength of OSB need to be identified for the specific I-joist before applying the method. In comparison, Software Package 2 provided online reasonably predicted the failure load for the "hole" test case, whereas Software Package 1 was not helpful. Software Package 1 did not provide the user with a failure load when the hole was close to the support. The testing setup using six-point bending was very effective for the purposes of this test and was a great benefit in eliminating lateral instability to achieve the failure modes required for testing the shear properties.

The OSB collar remediation technique worked very well and returned 8 of 12 series of joists to a strength that was statistically equivalent to the "no hole" condition. This method of remediation was more effective overall for long spans (with a larger moment: shear ratio) than for short spans. The maximum reduction of load from a joist with no hole to one with a hole was 49% for the long span and 58% for the short span. The construction adhesive used adequately transferred load into the patch and did not fail at a bond line. The presence of a web-to-web joint near a hole greatly influenced the load capacity. The OSB collar remediation technique was more effective in returning strength than the side LSL technique for only one of the test series. The side LSL remediation technique was generally more effective at returning the stiffness of the joist for both span lengths. The OSB collar method of remediation was less expensive and much easier to cut and install.

Recommendations

Future Work

Recommendations for future work on wood I-joists include the following:

1. Test the OSB collar remediation for 20–30 replicates but with a thicker OSB patch.
2. Test the remediation technique for creep and deterioration of the adhesive bond.
3. Test the remediation technique at the same location but with different size or shape holes.
4. Test I-joists with two holes in the web.

Practical Applications

The results from this research are very useful, given that they are used properly. The presented OSB collar patch is not meant to be a save-all solution to every hole condition. Fig. 12 presents the dimensions of the size and thickness of the OSB patch and recommendations for spacings from end supports and web-to-web joints. In Fig. 12(a), there must be a gap between the upper and lower OSB patches. If there is no gap and the two pieces are forced between the flanges, it is possible to cause additional stress on the web-to-flange connection, resulting in delamination.

Fig. 12(b) indicates the recommended thickness for the OSB patch and the direction of the screws. The screws are intended not to carry shear load but rather to apply pressure while the adhesive cures. This is a substitute for using blocking between joists or a carpenter's clamp.

Afzal et al. (2006) and manufacturers recommend keeping holes more than two diameters apart. This is to ensure that the stress state at the boundary of one hole has almost no influence on that of another. This reasoning can also be applied to a support condition [Fig. 12(c)], in which the high stresses occurring at the bearing can influence the stresses at the boundary of the hole. These restrictions

J. Mater. Civ. Eng., 2013, 25(12): 1898-1909

Downloaded from ascelibrary.org by OREGON STATE UNIVERSITY on 06/19/17. Copyright ASCE. For personal use only; all rights reserved.

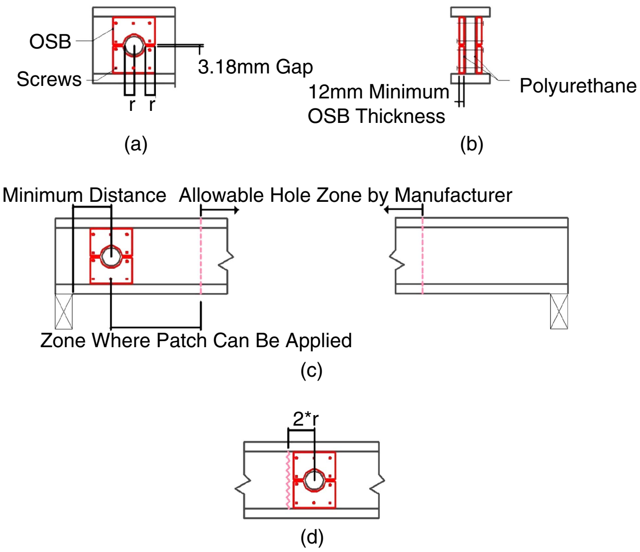

Fig. 12. OSB collar patch recommendations: (a) front view; (b) side view; (c) support distance and applicable patch location; (d) web-to-web joint distance

create a zone where the patch is applicable compared with the recommended zone by manufacturers, as seen in Fig. 12(c). An example of the new zone created for effective patches is compared in Table 7 for the hole size and joist depths used in testing. Another important result from these series of tests was the influence of the web-to-web joint on the failure load. Fig. 12(d) provides a recommended distance from the hole to the joint according to general observations from the testing.

The distances recommended for effective patches are based on the results of the two different span lengths tested. For the 241 and 356 mm (9.5 and 14 in.) depth joists, the OSB collar patch did not work effectively in terms of strength for the short span but was more effective for the long span, and it cannot be recommended without further testing. For the 406 mm (16 in.) depth joists, the OSB patch effectively provided capacity for both span lengths. The distance from the support shown in Table 7 is calculated as two times the diameter of the hole. This distance can be used because of the constant shear diagram in testing between the support and load closest to the support. This constant shear diagram in testing is more conservative than the linear one for the likely uniformly distributed load in practice.

The steps required for installation of the OSB collar patch are as follows:

1. Cut the OSB patch (OSB thickness is the same as I-joist web) to the depth of the I-joist web (interior-to-interior distance between flanges). Do not cut or notch the flanges.
2. Cut the OSB patch to a recommended length of two times the diameter of the hole.
3. Drill the hole into this patch by using a hole saw to create a uniform edge, as opposed to cutting with a reciprocating saw.
4. Cut the patch in half along the center of the hole, parallel to the I-joist flanges. This creates the top and bottom portion of the patch and also provides the minimum gap between patches.
5. Dispense PL Premium polyurethane adhesive from the tube and spread evenly across one side of the OSB patch. Place the OSB patch on both sides of the web above and below the hole. The minimum gap between the top and bottom piece of the patch is 3.2 mm (1/8 in.).

Table 7. Comparison of Limits for Hole Location with and without OSB Collar Patch

Joist depth, mm (in.)	Hole size, mm (in.)	Required distance from support to center of hole: With OSB collar, mm (in.)	Required distance from support to center of hole: Without OSB collar[a], mm (in.)
241 (9.5)	152 (6)	N/A	1,524 (60)
356 (14)	203 (8)	N/A	1,676 (66)
356 (14)	203 (8)	N/A	1,829 (72)
406 (16)	203 (8)	406 (16)	457 (18)
406 (16)	203 (8)	406 (16)	914 (36)
406 (16)	203 (8)	406 (16)	914 (36)

[a]From the manufacturer's hole chart.

6. Use Spax 5.2×51 mm (10×2 in.) course, yellow, zinc-plated, steel, flat-head, combination wood screws in an alternating pattern for one side of the patch. This will be three screws in one direction. Place two more screws on the opposite side of the web to tighten the bottom patch to the I-joist web. Repeat for the top portion of the patch, using a total of 10 screws. The pattern for the screws is shown in Fig. 12(a). Tighten until the screw head is embedded in the OSB and no gap remains between the OSB patch and I-joist web.

The tentative recommendations from this limited set of experiments are not meant to justify allowing holes to occur outside of the instructions of the manufacturer. However, the testing does provide tentative guidance on how to remediate holes that are outside these limits when they occur inadvertently. It is also still important to emphasize that there are no notches or cuts allowed into the flange, which is a very dangerous condition.

References

Afzal, M. T., Lai, S., Chui, Y. H., and Pirzada, G. B. (2006). "Experimental evaluation of wood I-joists with web holes." *For. Prod. J.*, 56(10), 26–30.

ASTM. (2010b). "Standard practice for sampling and data-analysis for structural wood and wood-based products." *D2915*, West Conshocken, PA.

ASTM. (2012). "Standard specification for establishing and monitoring structural capacities of prefabricated wood I-joists." *D5055*, West Conshohocken, PA.

Bower, J. E. (1966). "Elastic stresses around holes in wide-flange beam." *J. Struct. Div.*, 92(2), 85–101.

Chan, P. W., and Redwood, R. G. (1974). "Stresses in beams with circular eccentric web holes." *J. Struct. Div.*, 100(1), 231–248.

Cheng, R. J. (1996). "Design of OSB webbed I-joists with web opening." *Proc. of the Int. Wood Engineering Conf.*, Louisiana State University, Baton Rouge, LA, 134–141.

Clinch, R. W. (1993). "Effect of holes on static flexural stiffness of a wood composite I-beam." *For. Prod. J.*, 43(10), 23–28.

Guan, Z. W., and Zhu, E. C. (2009). "Finite element modelling of anisotropic elasto-plastic timber composite beams with openings." *Eng. Struct.*, 31(2), 394–403.

Huston, R., and Josephs, H. (2009). "Curved beams." *Practical stress analysis in engineering design*, 3rd Ed., Taylor & Francis Group, Boca Raton, FL, 199–210.

Knostman, H. D., Cooper, P. B., and Snell, R. R. (1977). "Shear force distribution at eccentric web openings." *J. Struct. Div.*, 103(6), 1207–1221.

LabView 2010 [Computer software]. National Instruments, Austin TX.

Lewis, W. C., Heebink, T. B., and Cottingham, W. S. (1944). "Effects of certain defects and stress-concentrating factors on the strength of tension flanges of box beams." *Rep. No. 1513*, Forest Products Laboratory, Madison, WI.

Morrissey, G. C., Dinehart, D. W., and Gary Dunn, W. (2009). "Wood I-joists with excessive web openings: An experimental and analytical investigation." *J. Struct. Eng.*, 135(6), 655–665.

J. Mater. Civ. Eng., 2013, 25(12): 1898-1909

Downloaded from ascelibrary.org by OREGON STATE UNIVERSITY on 06/19/17. Copyright ASCE. For personal use only; all rights reserved.

Pirzada, G. B., Chui, Y. H., and Lai, S. (2008). "Predicting strength of wood I-joist with a circular web hole." *J. Struct. Eng.*, 134(7), 1229–1234.

Polocoser, T. (2012). "Evaluation of remediation techniques for circular holes in the webs of wood I-joists." M.S. thesis, Oregon State Univ., Corvallis, OR.

Smith, C. B. (1944). "Effect of elliptic or circular holes on the stress distribution in plates of wood or plywood considered as orthotropic materials." *Rep. No. 1510*, USDA Forest Service, Forest Products Laboratory, Madison, WI.

Wang, S. (1994). "Shear behavior of OSB composite I-Beams with web openings." M.S. thesis, Univ. of Alberta, Edmonton, AB, Canada.

Wood I-Joist Manufacturers Association (WIJMA). (1999). "Establishing shear capacities for prefabricated wood I-joists with hole." ⟨http://i-joist.org/policies-publications⟩ (Feb. 28, 2012).

Zhu, E. C., Guan, Z. W., Rodd, P. D., and Pope, D. J. (2005a). "Buckling of oriented strand board webbed wood I-beams." *J. Struct. Eng.*, 131(10), 1629–1636.

Zhu, E. C., Guan, Z. W., Rodd, P. D., and Pope, D. J. (2005b). "Finite element modeling of OSB webbed timber I-beams with interactions between openings." *Adv. Eng. Softw.*, 36(11–12), 797–805.

Zhu, E. C., Guan, Z. W., Rodd, P. D., and Pope, D. J. (2007). "Structural behaviour of OSB webbed timber I-beams with openings." *J. Struct. Eng.*, 133(1), 145–149.

Downloaded from ascelibrary.org by OREGON STATE UNIVERSITY on 06/19/17. Copyright ASCE. For personal use only; all rights reserved.

J. Mater. Civ. Eng., 2013, 25(12): 1898-1909